Defence Science Journal, Vol. 63, No. 3, May 2013, pp. 262-270, DOI: 10.14429/dsj.63.2308

Mitigation of Mine Blast Loading by Collapsible Structures

I. M. Snyman

Council for Scientific and Industrial Research, Pretoria, South Africa
E-mail: isnyman@csir.co.za

ABSTRACT

This paper presents research results on the mitigation of mine blast loading by collapsible structures. A baseline test consisting of a test platform with a V-shape body exposed to the charge was executed, recording the imparted impulse and the deformation of the test item. A collapsible structure is added to the test platform and tested (two tests). By the law of conservation of momentum, similar peak imparted impulse values were obtained. However, the average imparted impulse reduced by between 16 % to 18% by adding this collapsible element in the load path. The average impulse is the total momentum transferred after the response of the damping system is filtered into the measurement system. The results are analysed with ANSYS AUTODYN and support the measured effects of the introduction of the mitigation measure.

Keywords: LandmineS, protection, ballistics, blast loading, collapsible structure

NOMENCLATURE

AISI	American iron and steel institute
AMV	Armoured modular vehicle
APC	Armoured personnel carrier
CSIR	Council for Scientific and Industrial Research
D:H	Diameter to height ratio
DBEL	Detonics and Ballistics Explosive Laboratory
DPSS	Defence, peace, safety and security
FCT	Flux-corrected-transport
kNs	Kilo-Newton second
LVDT	Linear variable differential transducer
mm	millimetre
msec	millisecond
PE4	Plastic explosive formulation 4
SIIMA	Scientifically instrumented impulse measuring apparatus

1. INTRODUCTION

The threat of landmines detonating below a vehicle is well known and is widely used in areas of conflict to the advantage of the military or civilian forces. Protecting a vehicle against such a threat is an ongoing research topic at various research institutes. At these institutes and universities, a wide range of protection measures are being investigated by various researchers that can be utilised against such a threat.

From the vehicles in use at present, it appears that the shape of the bottom part of the hull that is exposed to a landmines threat is still the most important aspect used for protection. An analysis of a number of land mine incidents and modifications to vehicles[1] confirm the design principles used since the seventies of the previous century. Vehicles below 20 tons use mainly a V-shaped hull with varying enclosed angles, from a sharp wedge shaped hull such as the CASSPIR[2] to a lesser pronounced wedge used in the RG31[3] or Mamba[4] Armoured Personnel Carrier. Flat bottom structures are normally used for vehicles over 20 tons such as the Patria Armoured Modular Vehicle[5], tanks and armoured fighting vehicles. In all these vehicles, the load path of the momentum transfer is directed along the sides to minimise impact on the occupants. The vehicle consists of a stiff outer shell, so that the occupants can be accommodated inside without obstacles (such as struts between the roof and the floor for additional strength). The mitigation of shock loading on these vehicles should be contained within the outer shell as not to compromise the protection of the occupants.

The loading mechanism of a detonating landmine below a vehicle is well-established[1]. The expanding gasses transfer the momentum to the exposed bottom section of the vehicle within a millisecond. The structure responds (by deformation for instance) within one or two milliseconds to this rapid momentum transfer. It is expected that the protection provided by the bottom section of a vehicle should be able to deal with such a rapid event.

Extensive research conducted by various research institutes published a variety of results. An example is the mine blast loading experiments[6] that provide an overview of this research in terms of the effects on damage and impulse by the soil conditions and the hull structure. Improvement of protection measures is normally company confidential and is very difficult to assess in isolation. The use of mitigation techniques in the improvement of the protection measures is not well documented.

Protection measures to mitigate the impact of a crash

Received 24 April 2012, revised 07 January 2013, online published 16 May 2013

on the passenger cabin are well advanced for usage in the commercial vehicle industry[7]. These measures are applicable to a frontal or side impact and occur over a few milliseconds. Some of these measures may become available if the time response range of the structures loaded by an explosive blast is altered to be within milliseconds instead of microseconds.

One way of doing just that is to have a particular structure (or component), that is exposed to the blast loading. Patents[8, 9] describe the absorption components of typical sections added to a vehicle designed for protection against land mines. The momentum of the blast is transferred to this section and subsequently to the remainder of the vehicle. The transfer of momentum is then reduced by collapsible elements. These elements may collapse by a variety of means and are not stipulated in the patents.

The same principle can be used as the collapsible structural elements in the front and rear end of a vehicle. In this paper, an experimental and computational analysis of such a protection principle for land mines is presented. The principle consists of three elements, namely a stiff structural section (a V-shape body) exposed to the explosive blast, a dedicated load path for the momentum transfer between this section and the remainder of the hull and a collapsible structure that interrupts (or prolongs) this momentum transfer. Any of the three elements currently in existence can be used in this combination.

2. TEST SET-UP

The three tests described below consist of two bodies subjected to a 0.667 kg PE4 charge (equivalent to C-4) with diameter to height ratio of 2, buried flush with the sand surface. The first test set-up consists of a half-scaled V-shape body, rigidly attached to an instrument to capture the imparted impulse (fixed configuration). This test acts as baseline for the following tests. The second and third test set-up consists of inserting a collapsible element between the V-shape structure and the instrument that captures the imparted impulse (collapsible configuration).

SIIMA captures the upward forces exerted by an explosive charge positioned below the moving mass (Fig. 1). SIIMA consists of a rigid frame with a suspended moving mass of approximately 8500 kg[10] and represents a gigantic mass-damper system. The test platform is added to the moving mass and sixteen load cells capture its response. The integration of the force time histories yield the impulse imparted to the moving mass. The exposed area of the moving mass is 1200 mm by 1200 mm. The soil pit (diameter 3000 mm and about 1500 mm deep) is filled with a specially formulated sand mixture. The experimental work was conducted at the DBEL outside Pretoria, South Africa.

The frame to which the test platforms are bolted onto is made out of steel channels 150 mm wide and with flanges of 100 mm. The frame is welded onto a 20 mm plate that is bolted onto the moving mass of SIIMA. The mass of the frame and plate is 348.5 kg.

2.1 V-shape Test Platform 1

The design of the V-shape test platform 1 is shown in Fig. 2. The body is rigidly attached to a frame that is in turn

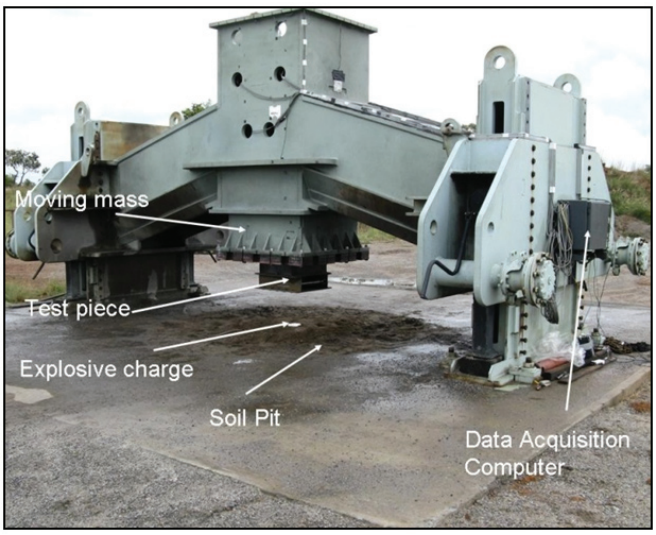

Figure 1. SIIMA on DBEL.

rigidly attached to the moving mass. The length and width of the blast facing V-shape is 600 mm. The height of the V is 200 mm and the enclosed angle of the V is approximately 112°. The ground clearance of the test platform lowest point is 200 mm. This type of design was first used in the CASSPIR vehicles [2], but with a smaller and hence sharper enclosed angle. Commercially graded mild steel of 8 mm thick is used with a capping (also 8 mm thick) at the bottom of the V for additional strength. The mass of the V-shape test platform 1 is 104.5 kg.

2.2 V-shape Test Platform 2 and 3

In order to investigate the usage of collapsible elements in the protection design, thin pre-formed plates were inserted between the V-shape body and the moving mass, the latter representing the vehicle structure. The design of such a collapsible structure is not straightforward and a simple (and probably very inefficient) design was chosen to illustrate the principle. The insertion of this element is a deliberate step to

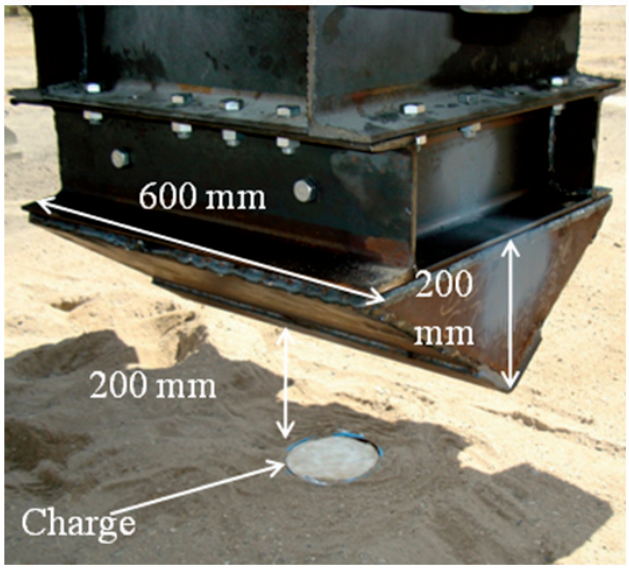

Figure 2. The set-up of the V-shape test platform.

interrupt the load path followed by the force exerted by the landmine. This is similar to protecting the occupants inside the cabin of a crashing vehicle.

The exposed protection element (the V-shape structure) to the landmine is very stiff and will not compromise the dedicated load path (via the collapsible elements).To have the same standoff distance, the height of the V-shape body was reduced by 50 mm to incorporate the height of the collapsible plate element. The design of the collapsible plate is simple (for the test) but it is anticipated that the design can become more intricate to accommodate the load scenario of a mine-protected vehicle.

Figure 3 shows the set-up of the test platform with a collapsible preformed plate. The collapsible pre-formed plate is inserted between the frame and the V-shape body and is clearly visible. The height of the collapsible pre-formed thin plate is 50 mm and the thickness is 2 mm. The mass of the test platform is 68.5 kg. The ground clearance of the test platform lowest point is 200 mm. The sand was wet, but not saturated. Because of the special soil formulation, this type of wet soil increases the impulse marginally[11].

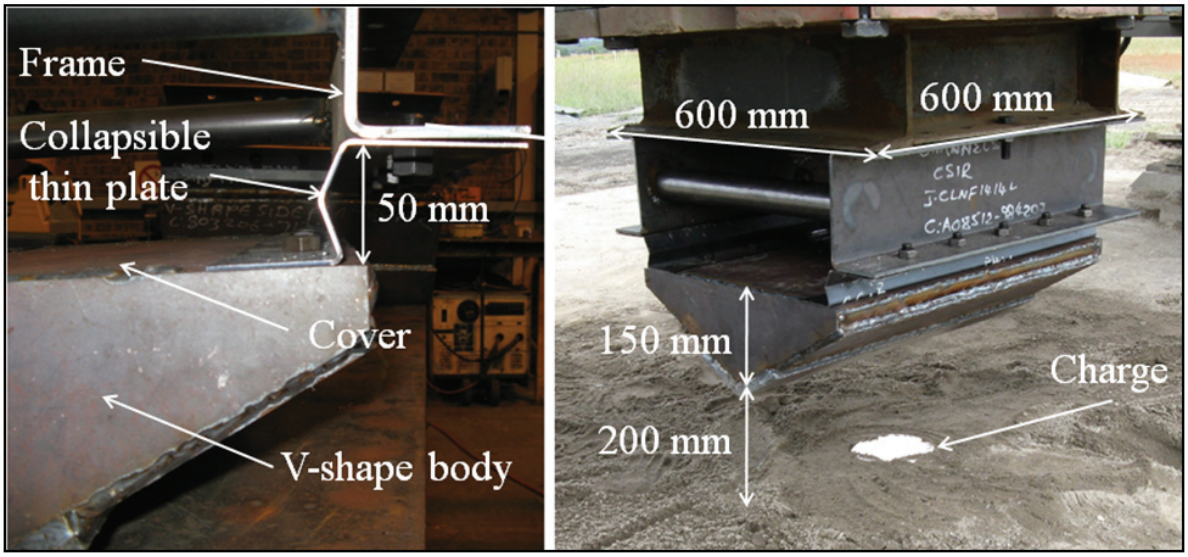

Figure 3. The V-shape test-platform 2 and 3 with the collapsible preformed plate.

3. MEASURING THE IMPARTED IMPULSE

SIIMA captures the force with sixteen load cells exerted by the moving mass. Figure 4 shows the total force exerted by the moving mass on the load cells (tied to a rigid body) for the test below with platform 3. Note the oscillatory nature of the force due to the response of the suspended mass (spring-mass damper system). The function of the dampers is to absorb the energy and reduce the motion of the moving mass after the loading event. The region of interest is therefore the peak force and the area below. The time zero on the horizontal axis is the time of detonation. The peak force occurs at approximately 20 msec after detonation.

Integration of the force over time yields the imparted impulse of the buried charge below the moving mass. Figure 5 shows the imparted impulse over time. Note the oscillatory nature of the imparted impulse. The first peak represents the area under the first peak of the force over time in Fig. 4 and up to about 20 msec. This is considered the momentum transferred to the system by the blast loading. The remainder of the curve represents the impulse as the spring damper system absorbs the energy. The average impulse refers to the total momentum transferred between the two sets of bump stops that dampen the motion of the moving mass. The results in the sections below refer to the peak and average imparted impulse.

The vertical displacement of the moving mass is very little and is captured by a linear variable differential transformer. The peak displacement is 0.85 mm and is shown in Fig. 6. The response of the moving box to the blast load takes longer as the maximum displacement occurs at approximately 280 msec after detonation.

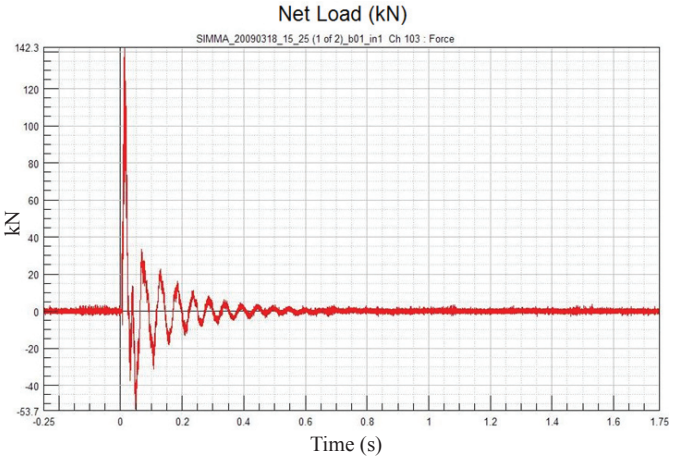

Figure 4. The total force captured by the load cells in SIIMA for Platform 3.

4. TEST RESULTS

Three tests were executed on DBEL. The results are briefly described below in terms of deflection, imparted impulse and peak force.

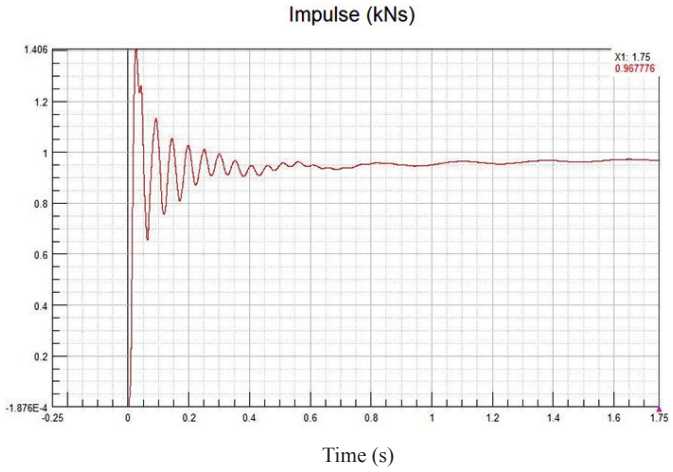

Figure 5. The imparted impulse captured by SIIMA for platform 3.

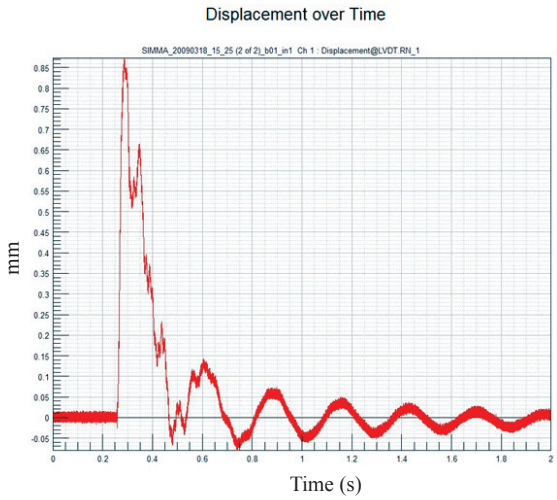

Figure 6. The upward displacement of the moving mass of SIIMA for Platform 3.

4.1 V-shape Test Platform 1

Figure 7 shows the damage to the V-shaped body after the test. The exposed bottom plates and capping has deformed slightly at the centre of the V. The deflection of the mid-point (with the capping) of the V-shape is 12 mm. The deflection of the side of the V is 25 mm (measured perpendicular on the surface). The peak imparted impulse captured by SIIMA is 1.475 kNs and the average imparted impulse is 1.015 kNs. The peak force is 162 kN and the maximum displacement is 0.85 mm.

4.2 V-shape Test Platform 2 and 3

The test platforms after the detonation are shown in Fig. 8 and the results are very similar. The preformed plate has folded up as a result of the upward motion of the V-shape body. Once the preformed plate folded close, the upward momentum of the V-shaped body pushed against the frame. The result is that the body was pushed into the frame, as shown in Fig. 8. This implies that the design of the collapsible element is not optimal. However, it clearly illustrates the effect of the momentum transfer.

The deformation of the V-shaped platform 2 at the centre of the V is 14 mm. The deflection of the mid-point (with the capping) of the V-shape is 14 mm. The deflection of the side of the V is 35 mm (measured perpendicular on the surface). The peak imparted impulse captured by SIIMA is 1.472 kNs and the average imparted impulse is 0.852 kNs. The peak force is 153.2 kN and the maximum displacement is 0.85 mm. The V-shape element displaced about 16 mm into the frame.

The deformation of the V-shaped platform 3 at the centre of the V is 19 mm. The deflection of the mid-point (with the capping) of the V-shape is 19 mm. The deflection of the side of the V is 35 mm (measured perpendicular on the surface). The peak imparted impulse captured by SIIMA is 1.406 kNs and the average imparted impulse is 0.832 kNs. The peak force is 42.3 kN and the maximum displacement is 0.87 mm. The V-shape element displaced is also about 16 mm into the frame.

Figure 7. Damage to the V-shape body platform 1.

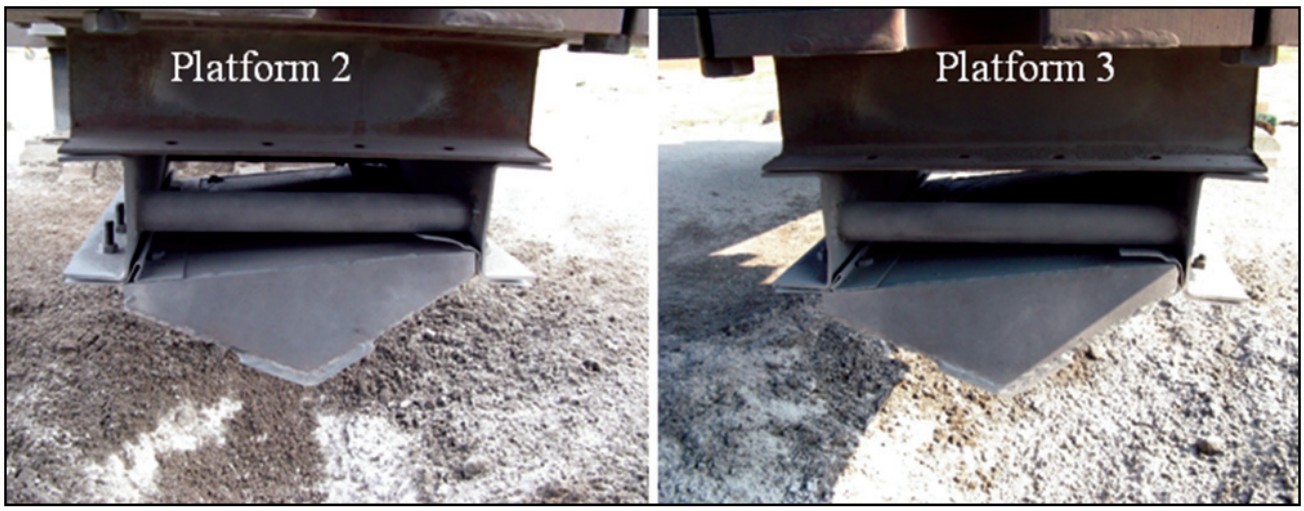

Figure 8. The collapse of the preformed plate is clearly visible.

4.3 Discussion

Table 1 contains a summary of the measurements of the tests. The damage to the V-shape body increased from the rigid set-up (platform 1) to the frangible set-up (platform 2 and 3). The reason may be ascribed to a number of factors of which the important one is that the material for platform 2 and 3 is from a different batch as platform 1. Commercially graded mild steel have yield point over a range from 180 MPa to 240 MPa. Equally important, the body in platform 2 and 3 is slightly smaller and lighter as the one used in platform 1. It will therefore deform more as the area on which the pressure acts is smaller.

Table 1. Summary of the test results

Damage	Platform 1	Platform 2	Platform 3
Centre (mm)	12	14	19
Side (mm)	25	35	35
Average impulse (kNs)	1.015	0.852	0.832
Peak impulse (kNs)	1.475	1.472	1.406

The change in imparted impulse is of interest. The average impulse (that incorporates the damping elements in SIIMA) was reduced considerably (by more than 15 per cent) while the peak imparted impulse remained the same. This phenomenon is investigated by computational analysis and discussed more deeply in the following section.

The average imparted impulse of the three tests is in the same order of the impulses obtained by a different method [6] with 0.625 kg Comp B, depth of burial 50 mm and ground clearance 200 mm for a V-shape plate with enclosed angle of 120°. The plate displacement was used to obtain the imparted impulse.

5. COMPUTATIONAL ANALYSIS

The computational analyses had been done with ANSYS AUTODYN on a Dell Precision dual 2.6 GHz Pentium processor. ANSYS AUTODYN solves the conservation laws of momentum, mass and energy at every time step (determined by the size of the mesh) subject to boundary and initial conditions. An appropriate material model solves the equation of state, strength and failure of the material[13].

The computation of the damage and imparted impulse of each experiment were analysed and compared with the measurements from each test. The computational model of SIIMA consists of the moving mass, the air surrounding it and the soil pit. The moving mass is free in air and not constraint in any way and the damping mechanisms are not included in the model. The modelling approach is similar to the ones followed previously[11,12]. Added to the moving mass is the test platform modelled with shell elements. The computational modelling of the event up to five milliseconds captures the momentum transfer to the moving mass and the response of the test platforms. Quarter symmetry is used in setting up the computational models in order to reduce computation time with the effect that asymmetrical phenomena will not be calculated. Each of the computations took 18 hrs to complete.

5.1 Computational Model

The air and explosive gas are modelled with an Euler-flux corrected transport (FCT) solver, which uses only the ideal equation of state. The cubic element has a side length of 15 mm. The explosive is modelled as compressed air with internal energy and density equivalent to C-4 (an explosive very similar to PE4). The expansion of the gases is calculated using the ideal gas equation of state. The sand in the soil pit and the moving mass are modelled with the Lagrange solver, using eight node elements. A graded mesh is used with smallest cubic element with side length of 6 mm. The cubic elements in the moving mass have a side length of 20 mm. The test platforms are modelled with the Lagrange solver, using two dimensional shell elements (size 20 mm by 20 mm).

The Euler-Lagrange interaction algorithm controls the interaction of the expanding gas in the Euler-FCT mesh. The Lagrange interaction algorithm using a gap size to determine the onset of interaction controls the interaction of the materials modelled with the Lagrange meshes. The materials used for the computations are given in Table 2. The material parameters are

obtained from published data where possible and are contained in the AUTODYN material library.

The computational model set-up for test platform 1 is shown in Fig. 9 (reflected about the symmetry planes). The model shows the sand pit, explosive buried flush to the surface, the test platform, frame and moving mass. The surrounding air is not shown.

plate is 2 mm thick and 50 mm wide. The modelling of the frame is slightly different from the one used in the test. In the test, a cylindrical beam is used instead of a channel.

The collapse of the preformed plate is shown in Fig. 13 at various times. At 750 microseconds after detonation, the plates are starting to collapse. The flow of expanding explosive gases are deflected by the V-shape body and the interaction with the surface provides enough upward directed force.

Table 2. The material models and parameters used by the computational models

Material	Parameters	Equation of state	Strength	Failure
Air	Ambient air at 15°C	Ideal gas	-	-
PE4 charge	Hot compressed air for C4	Ideal gas	-	-
Moving mass	AISI 1006 steel [14]	Shock	Johnson Cook	Johnson Cook
Test platform plates	AISI 1006 steel [14]	Linear	Johnson Cook	Johnson Cook
Sand in soil pit	Sand [15]	Linear	Drucker-Prager	Hydro-dynamic

5.2 V-shape Platform 1

The V-shape test platform computational model is shown in Fig. 10 reflected about the symmetry planes and the thickness of the shell elements for display purposes. The capping of 8 mm thick is clearly visible.

The computational result (shown in Fig. 11) at 5 msec agrees fairly well with the experimental test result. The deflection is calculated as 12.6 mm and the deflection of the side is 26 mm. Some damage to the frame is visible, while minimal damage to the frame occurred in the test. The final mid-point deflection of the V-shaped plate and the deflection of the side plates making up the V are shown in Table 3.

The calculated imparted impulse agrees well with the peak imparted impulse but over-predicts the average measured impulse with more than 30 per cent. This is because the damping elements of SIIMA are excluded from the computational model.

The agreement between the computational and experimental results paved the way to investigate the response of the body in the other two tests.

5.3 V-shape Platform 2

The computational model showing the preformed collapsible component is given in Fig. 12, with the mesh reflected about the symmetry planes. The relative thicknesses of the various plates are also shown. The collapsible mild steel

Table 3. The computational and experimental results of platform 1

Damage	Computation at 3 msec	Measure-ment	Difference
Centre (mm)	12.6	12	-5%
Side (mm)	26.0	25	-4%
Average impulse (kNs)	1.349	1.015	-33%
Peak impulse (kNs)		1.475	9%

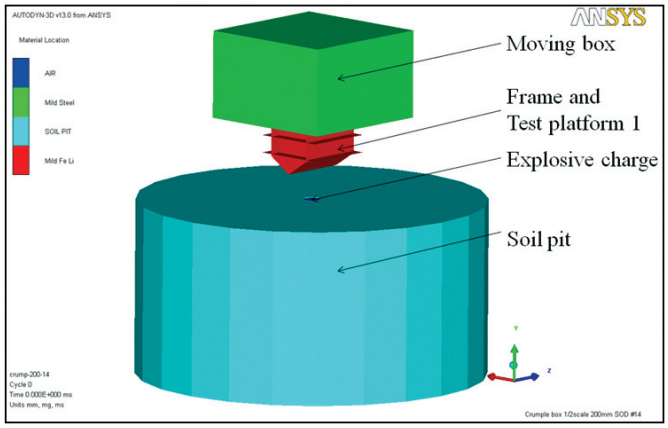

Figure 9. The computational model with test platform 1.

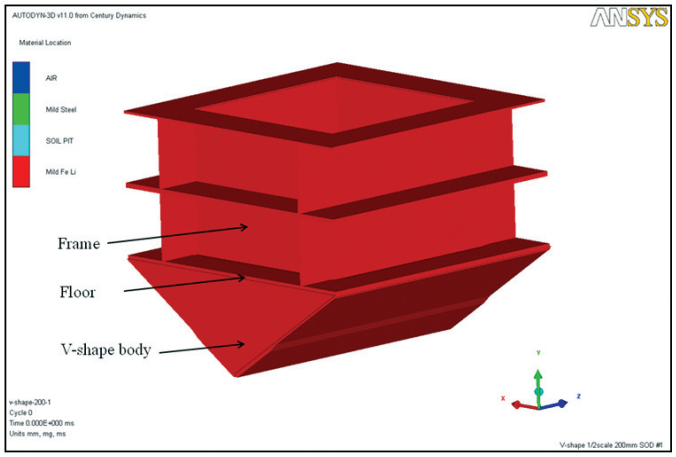

Figure 10. The set-up of the V-shape test platform 1.

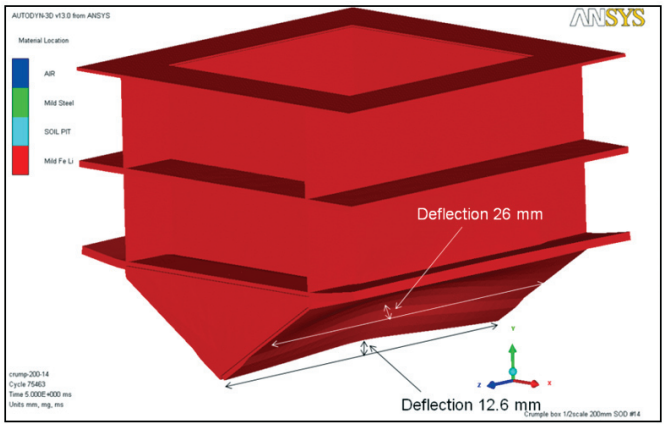

Figure 11. The computation of the damage to the V-shape box (model reflected about symmetry planes).

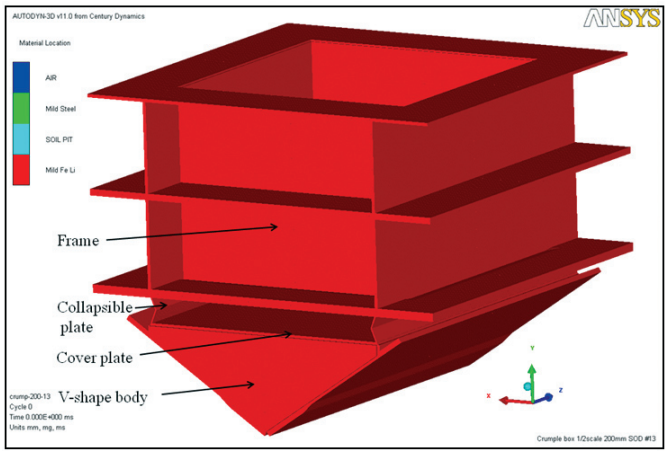

Figure 12. The computational model with the preformed collapsible plate (reflected about the symmetry planes).

The upward motion of the body causes the collapse of the preformed plates. At 1.5 msec after detonation, the preformed plates have collapsed sufficiently to affect the impulse and the flow of explosive gases around the V-shaped body. At 5 ms, the computation was stopped as the preformed plates collapsed completely.

The computational result as shown in Fig. 14 at 5 msec agrees fairly well with the experimental test result. The preformed plate completely collapsed and the body is pressing against the frame. The symmetries employed in the computational model exclude any asymmetrical response (as is apparent from the test results in Fig. 8). The deflection of the V-shape is calculated as 13.6 mm and the deflection of the side plate is 30 mm.

The final mid-point deflection of the V-shaped plate and the deflection of the side plates making up the V are shown in Table 4. The deflection of the plates of the body is under predicted by about 40 per cent. The deformation of the body from experimental results of platform 2 and 3 differs from the results of platform 1. The material used to construct the bodies is from different batches of commercially graded mild steel and may have lead to the differences in values.

The calculated imparted impulse agrees well with the peak imparted impulse but over-predicts the average measured impulse with more than 30 per cent. This is because the damping elements of SIIMA are excluded from the computational model.

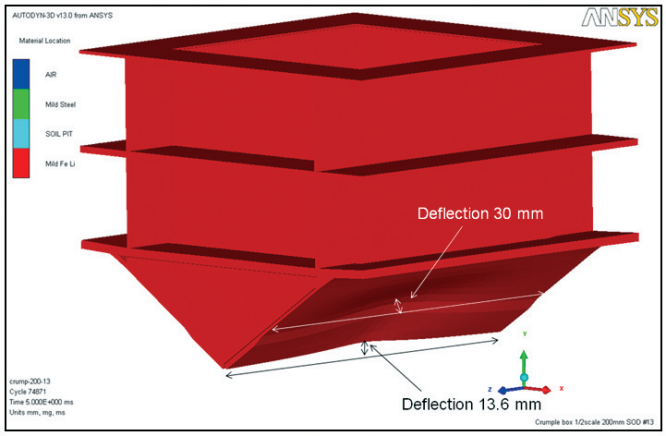

Figure 14. The computation of the damage to the V-shape box (model reflected about symmetry planes).

Table 4. The computational and experimental results of platform 2

	Computation	Measurement	
Damage	at 5 ms	Platform 2	Platform 3
Centre (mm)	13.6	14	19
Side (mm)	30	35	35
Average impulse (kNs)	1.349	0.852	0.832
Peak impulse (kNs)		1.472	1.406

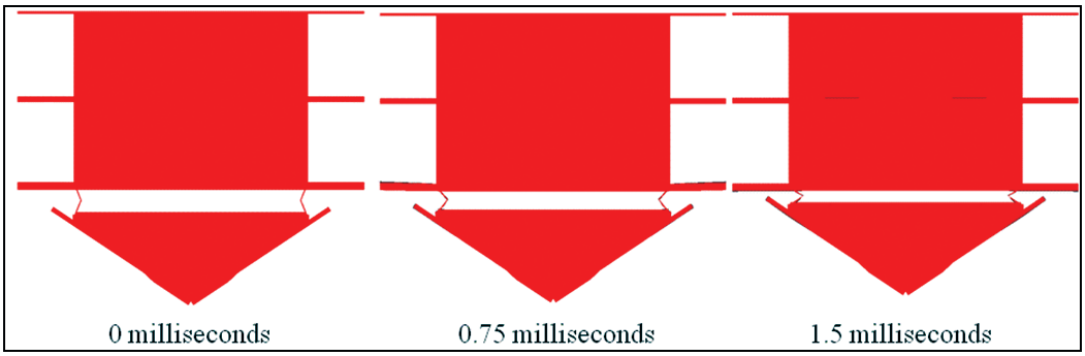

Figure 13. The side view showing the collapse of the preformed plates section.

5.4 Discussion

The difference between the calculation of the deflections of platform 2 and 3 and the measured values can be ascribed to a number of factors noted previously in section 4.3. The body in platform 2 and 3 is slightly smaller and lighter as the one used in platform 1 and it will slightly deform more as the area on which the pressure acts is smaller. This is supported by the computational analysis.

The upward motion was such that the preformed plate collapsed as the experimental evidence in Figure 8 indicates and the computational analysis in Fig. 13 shows. The computational analysis calculated the average upward velocity of the centre of gravity of the blast facing V-shape body for both the collapsible configuration and the fixed configuration. Figure 15 shows the upward velocity of two components of each set-up. For the fixed body as shown in Fig. 9, the upward velocity of the V-shape body and the floor is shown and for the collapsible structure, the V-shape body and the cover as shown in Fig. 12. It is evident that the collapsible plate allows the V-shape body and cover to decelerate at a slower pace as for the fixed case. At about 5 msec, the upward velocity is almost zero for all the components. Note the high initial velocity attained for the V-shape body, namely 25 m/s. The fixed configuration oscillates about zero from about 1.5 msec while the collapsible configuration decelerates and displaces upward.

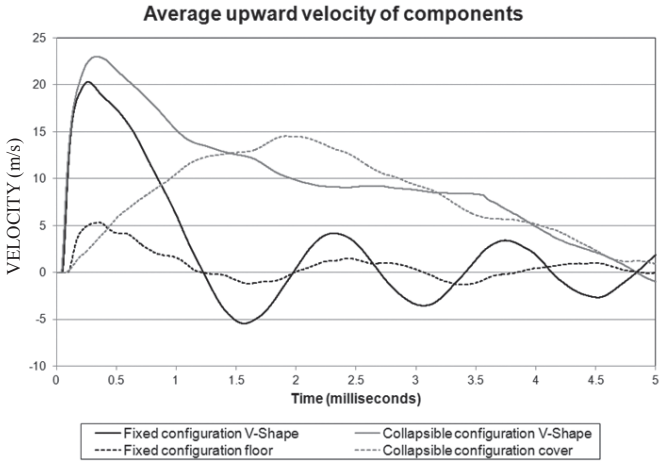

Figure 15. The average upward velocity of centre of gravity of the components of the bodies.

The centre of gravity of the collapsible configuration displaces 50 mm in five msec, as is evident from Fig. 16. The centre of gravity of the fixed configuration displaces about 12 mm in one msec and oscillates about this displacement as the moving mass is preventing any further upward motion. This 12 mm upward displacement is due to the deformation of the V-shape component facing the blast. The 50 mm displacement of the collapsible configuration contains also an element of deformation of the V-shape component facing the blast.

Let us turn now to the computation of the imparted impulse (or momentum transfer) that agrees with the peak impulse recorded by SIIMA. The calculation of the peak impulse value under predicts the measured values by not more than 10 per cent (the worst case). By the law of conservation

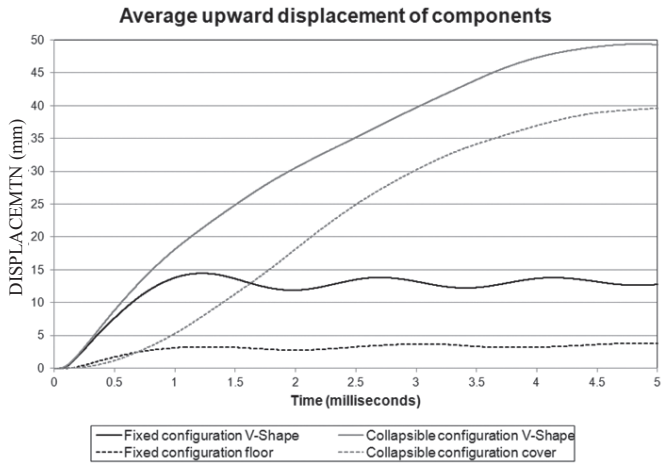

Figure 16. The average upward displacement of components of the bodies.

of momentum, the total imparted impulse time histories are very similar for the two configurations as is evident from Fig. 17. However, the composition of the total imparted impulse differs substantially between the two configurations. The trend is similar to the upward velocities depicted in Fig. 15. The momentum transfer to both test platforms is a maximum before 0.5 msec, after which the momentum transfer to the moving mass of the fixed configuration is completed after about 1.5 msec. The momentum transfer to the moving mass of the collapsible configuration is completed after five milliseconds.

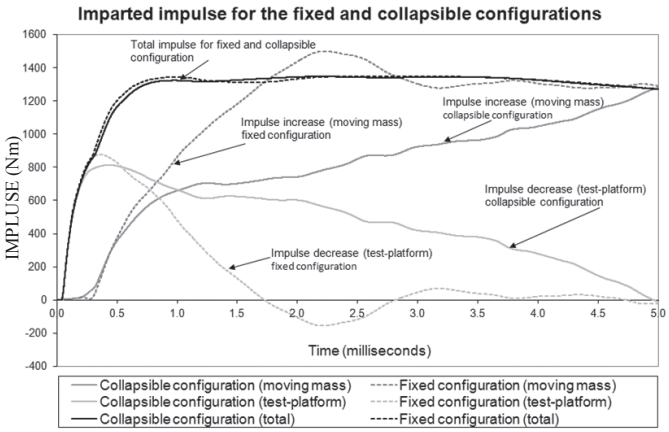

Figure 17. The imparted impulse time histories of the fixed and collapsible configurations.

6. CONCLUSION

A summary of the data captured by SIIMA for the three test platforms are shown in Table 5. By the law of conservation of momentum, similar peak imparted impulse values are expected. The average imparted impulse, however, was reduced by between 16 per cent to 18 per cent by adding a collapsible element in the load path. This trend is despite the fact that a lower D:H ratio was used for the explosive charge (which gives a lower impulse of about 5 per cent) and the condition of the sand in the soil pit (wet for these tests and dry for the Test #3). Wet soil increases the impulse marginally[11] for buried charges.

The average impulse is a result of the total imparted

Table 5. Summary of measured imparted impulse data

	Test Platform 1	Preformed plate	
		Test #2	Test #3
Peak impulse (kNs)	1.475	1.472	1.406
Average impulse (kNs)	1.015	0.852	0.832
Difference (%)		16%	18%

impulse to the measurement system represented by SIIMA. In other words, the total momentum transferred after the response of the damping system is filtered into the motion of the moving mass. The response of the gigantic spring mass damper system to an explosive charge can be interpreted as the response of a vehicle with a body attached to the bottom section. It is evident that the collapsible configuration translates into a reduction of momentum transfer of the complete vehicle by 16 per cent to 18 per cent.

The collapsible configuration is by no means optimal. The structural engineer should optimise the collapsible configuration according to the vehicle mass, the integration of the body into the vehicle structure and the stroke length of the collapsible element.

ACKNOWLEDGEMENT

The support of Mr DK Engels, Manager of Landward Sciences for the research and the financial contribution of the CSIR is gratefully acknowledged. The staff assisting with the execution of the tests and measurements is thanked for their continual support.

REFERENCES

1. Ramasamy, A.; Hill, A.M.; Masouros, S.D. Gordon, F.; Clasper, J.C. & Bull, A.M.J. Evaluating the effect of vehicle modification in reducing injuries from landmine blasts. An analysis of 2212 incidents and its application for humanitarian purposes. Accident Analysis and Prevention, 2011, 43(), 1878– 886.
2. Casspir. http://en.wikipedia.org/wiki/Casspir (Accessed on 26 June 2009)
3. RG-31 Nyala. http://en.wikipedia.org/wiki/RG-31 Nyala (Accessed on 26 June 2009)
4. Mamba_APC. http://en.wikipedia.org/wiki/Mamba_APC (Accessed on 26 June 2009)
5. Patria_AMV. http://en.wikipedia.org/wiki/Patria_AMV (Accessed on 26 June 2009)
6. Anderson, C.E.; Jr, Behner, T. & Weiss, C.E. Mine loading experiments. *Int. J. Impact Eng.,* 2011, **38**(8-9), 697-706.
7. Jones, N. & Wierzbicki, T. (Eds). Structural crash worthiness and failure, Elsevier, 1993.
8. Fransolet, C.; Ackerman, S.W.; Steenkamp, R. & Nel, D. Vehicle body portion. Australian patent 703 896 B2, 1 April 1999.
9. Barbe, Y.; Bettencourt, B. & Wagnez, L. Protection device for the floor of a land vehicle. US Patent 2008/0349531, 14 February 2008.
10. Snyman, I. M. & Reinecke, J. D. Measuring the impulse from an explosive charge. Paper presented at the Ballistics Symposium South Africa, Denel-OTB, Bredasdorp, 15-16 Aug 2006.
11. Reinecke, D. J.; Snyman, I. M.; Ahmed, R. & Beetge, F. J. A Safe and Secure S. A.: Blast characterization through impulse measurements. Paper presented at the 2nd Biennial Conference CSIR, Pretoria, RSA, 17-18 Nov 2008.
12. Smith, P. F.; Snyman, I. M. & Mostert, F. J. Comparison of methods to measure the blast impulse of an explosive charge. Paper presented at the 24th International symposium on Ballistics, 22-26 Sep 2008, New Orleans, USA.
13. Zukas, J.A. Introduction to hydrocodes. *In* Studies in applied mechanics, Vol. 49, Elsevier, 2004.
14. Johnson, G.R. & Cook, W.H. A constitutive model and data for metals subjected to large strains, high strain rates and high temperature. Paper presented at the 7th International Ballistics Symposium, The Hague, The Netherlands, April 1983, pp. 541– 47.
15. Heymann, G. Report on soil parameters at the Paardefontein landmine experiment site. Heymann, G. Report No. 23204. 23 Feb 2004.

Contributor

Dr Izak Marius Snyman obtained his MSc and PhD in Applied Mathematics in 1978 and 1982, respectively from the University of South Africa. Currently working as a Principal Scientist and Research Group Leader with regard to the development of protection techniques against threats such as blast and impact. He is also responsible for the modelling and simulation of complex phenomena of short time duration and large deformations (such as explosions, impact or ballistic impact). The solution involves finite element and finite difference methods used in a hydrocode such as ANSYS AUTODYN. He has published more than 39 research papers.